Contribution from the Department of Chemistry, Faculty of Science,
Tohoku University, Aoba-ku, Sendai 980, Japan

Electrochemical Behavior of $[Cp'_2Fe_2S_4]$ and $[Cp'_2Fe_2S_4](PF_6)_2$ ($Cp' = \eta^5$-C_5Me_5): Structural Change of the Fe_2S_4 Core Accompanied by a Change of Redox State

Shinji Inomata, Hiromi Tobita, and Hiroshi Ogino*

Received January 15, 1991

Bulk electrolysis of $Cp'_2Fe_2S_4$ in 0.1 M NH_4PF_6 in CH_3CN at a peak potential for a one-electron-oxidation wave (+0.30 V vs SCE) gives a two-electron-oxidation product $[Cp'_2Fe_2S_4](PF_6)_2$ in high yield, where an Fe_2S_4 core with a bidentate and a doubly bidentate μ-S_2 ligands in the neutral species (A type species) changes to one with two doubly bidentate μ-S_2 ligands in the dicationic species (B type species) during oxidation. Electrochemical and spectroscopic studies on the redox behavior of these neutral and dicationic species have shown that a total of six species, i.e. a neutral complex, a monocation, and a dication with A-type cores and the same with B-type cores, participate in the redox reactions between $[Cp'_2Fe_2S_4]$ and $[Cp'_2Fe_2S_4](PF_6)_2$. The one-electron-oxidation potential of $[Cp'_2Fe_2S_4]$ ($E_{1/2}$ = +0.25 V vs SCE) is more positive than the one-electron-reduction potential of $[Cp'_2Fe_2S_4](PF_6)_2$ ($E_{1/2}$ = +0.15 V vs SCE), and the interconversion between A and B geometries of the Fe_2S_4 core is fast for monocations. Thus, an ECE-type process operates for the formation of $[Cp'_2Fe_2S_4](PF_6)_2$ from $[Cp'_2Fe_2S_4]$. The equilibrium constant for the electron transfer between $[Cp'_2Fe_2S_4]$ and $[Cp'_2Fe_2S_4](PF_6)_2$ has been estimated.

Introduction

A reversible structural change accompanying electron-transfer reactions is one of the intriguing and rapidly growing areas in the redox chemistry of metal complexes.[1-5] However, only very limited types of complexes have been studied so far, especially in the case of dinuclear and polynuclear complexes.[6-10]

Organometallic complexes with a general formula $Cp^*_2M_2S_4$ (Cp^* = substituted cyclopentadienyl, M = transition metal) make a unique class with a remarkable variety in the structure of their M_2S_4 core.[11-13] Comparing these complexes containing different transition metals, it looks evident that the number of valence electrons on the metals is an important factor in determining the core structure. A simple reason may be that the Cp*M's with different valence electrons require contribution of the different number of electrons from the coordinated four sulfur atoms, which then respond by changing their coordination mode. Instead of changing metals, the oxidation or reduction of complexes also changes the number of valence electrons on the metal centers and is expected to cause a similar structural change. Nevertheless, the relationship between the redox behavior of $Cp^*_2M_2S_4$ and their structures has not been investigated until recently.

Brunner et al.[14] and we[15] have recently reported that the diiron complex $Cp'_2Fe_2S_4$ ($Cp' = \eta^5$-C_5Me_5) with bidentate and a doubly bidentate μ-S_2 ligands changes by two-electron oxidation to the dication with two doubly bidentate μ-S_2 ligands (eq 1). A mechanism involving a monocationic intermediate and its disproportionation to neutral and dicationic species has been proposed on the basis of the cyclic voltammograms at room temperature.

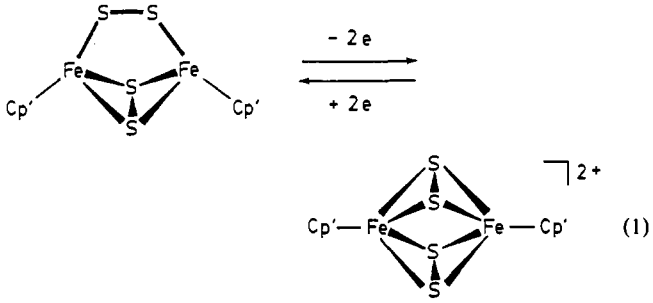

(1)

However, by a more detailed electrochemical study including low-temperature measurements, we found that six species, i.e. two neutral complexes, two monocations, and two dications, participate in the redox reactions between the isolated $Cp'_2Fe_2S_4$ and $[Cp'_2Fe_2S_4]^{2+}$.

We show here the details of the electrochemical studies on both $Cp'_2Fe_2S_4$ and $[Cp'_2Fe_2S_4](PF_6)_2$ in various conditions as well as the UV–visible, ^1H NMR, and ESR spectroscopic investigations.

Experimental Section

Chemicals. $[Cp'_2Fe_2S_4]$ was prepared by the method described by Brunner et al.[16] Tetra-*n*-butylammonium tetrafluoroborate (TBAB) was obtained from Tokyo Chemical Industry Co., Ltd., and recrystallized from ethanol. Ammonium hexafluorophosphate was purchased from Aldrich Chemical Co., Inc. and was used without further purification. Acetonitrile was dried by distillation from phosphorus pentoxide (twice) and then from calcium hydride. Dichloromethane was dried by distillation from calcium hydride.

Electrochemical Measurements. Electrochemical measurements were performed with a Fuso Model 311 potentiostat and a Model 321 function generator. Measurements were made with a three-electrode system with a platinum rod working electrode, a platinum coil auxiliary electrode, and a saturated calomel reference electrode (SCE). A measured solution was coupled through a salt bridge filled with a 0.1 M TBAB solution to the reference electrode. In the case of low-temperature measurement, a cell with a cooling jacket was used and temperature-controled methanol was circulated through it to maintain the cell at −30 to −35 °C. TBAB was used as the supporting electrolyte and was dissolved in acetonitrile or dichloromethane to make 0.1 M solutions.

Spectroscopic Measurements. ^1H NMR spectra were measured on a Varian XL-200 spectrometer. ESR spectra were obtained on a JEOL JES-FE2XG spectrometer. Electronic spectra were recorded on a Shimadzu UV-265 spectrophotometer. IR spectra were recorded on a JASCO R-810 spectrophotometer. Mass spectra were measured on a Hitachi M-52 spectrometer.

Preparation of $[Cp'_2Fe_2S_4](PF_6)_2$ by Electrolysis of $[Cp'_2Fe_2S_4]$. A 0.1 M NH_4PF_6 solution in acetonitrile (100 mL) was placed in the electrolysis cell and deoxygenated with nitrogen. $[Cp'_2Fe_2S_4]$ (210 mg, 0.411

(1) Geiger, W. E. In *Progress in Inorganic Chemistry*; Lippard, S. J., Ed.; J. Wiley: New York, 1985; Vol. 33, p 275.
(2) Evans, D. H.; O'Connell, K. M. In *Electroanalytical Chemistry*; Bard, A. J., Ed.; Marcel Dekker: New York, 1986; Vol. 14, p 113.
(3) Evans, D. H. *Chem. Rev.* **1990**, *90*, 739.
(4) Edwin, J.; Geiger, W. E.; Rheingold, A. L. *J. Am. Chem. Soc.* **1984**, *106*, 3052.
(5) Rieke, R. D.; Rich, W. E.; Willeford, B. R.; Poliner, B. S. *J. Am. Chem. Soc.* **1975**, *97*, 5951.
(6) Tulyathan, B.; Geiger, W. E. *J. Am. Chem. Soc.* **1985**, *107*, 5960.
(7) Gaudiello, J. G.; Wright, T. C.; Jones, R. A.; Bard, A. J. *J. Am. Chem. Soc.* **1985**, *107*, 888.
(8) Moulton, R. D.; Chandler, D. J.; Arif, A. M.; Jones, R. A.; Bard, A. J. *J. Am. Chem. Soc.* **1988**, *110*, 5714.
(9) Lyons, L. J.; Tegen, M. H.; Haller, K. J.; Evans, D. H.; Treichel, P. M. *Organometallics* **1988**, *7*, 357.
(10) Mevs, J. M.; Geiger, W. E. *J. Am. Chem. Soc.* **1989**, *111*, 1922.
(11) Wachter, J. *J. Coord. Chem. B* **1987**, *15*, 219.
(12) Wachter, J. *Angew. Chem., Int. Ed. Engl.* **1989**, *28*, 1613.
(13) Tremel, W.; Hoffmann, R.; Jemmis, E. D. *Inorg. Chem.* **1989**, *28*, 1213.
(14) Brunner, H.; Merz, A.; Pfauntsch, J.; Serhadli, O.; Wachter, J.; Ziegler, M. L. *Inorg. Chem.* **1988**, *27*, 2055.
(15) Ogino, H.; Tobita, H.; Inomata, S.; Shimoi, M. *J. Chem. Soc., Chem. Commun.* **1988**, 586.
(16) Brunner, H.; Janietz, N.; Meier, W.; Sergeson, G.; Wachter, J.; Zahn, T.; Ziegler, M. L. *Angew. Chem., Int. Ed. Engl.* **1985**, *24*, 1060.

0020-1669/91/1330-3039$02.50/0

mmol) was added, and the mixture was deoxygenated again and electrolyzed with stirring. The voltage was slowly increased from 0.0 to +0.30 V vs SCE. Electrolysis was continued (for about 2 h) until the current decreased to almost zero. The deep green solution was transferred to a round-bottomed flask through a filter to remove insoluble materials, and was concentrated to 3–4 mL in vacuo. The residual solution was stored under nitrogen in a refrigerator overnight, and the microcrystalline, dark green product together with colorless crystals of excess NH_4PF_6 was collected on a frit, thoroughly washed with water to remove NH_4PF_6, then washed with ether, and dried. Recrystallization under nitrogen from acetonitrile–ether gave 238 mg (0.297 mmol, 72%) of $[Cp'_2Fe_2S_4](PF_6)_2$ as dark green crystals: ^1H NMR (CD_3COCD_3) δ 1.59 (30 H, s, Me); IR (KBr) 1475 m, 1423 m, 1380 m ($\delta(CH_3)$), 839 s, 556 s (ν(P–F)), 540 sh (ν(S–S)) cm^{-1}; MS m/z 510 ($[Cp'_2Fe_2S_4]^+$); UV–vis (CH_3CN) λ_{max}/nm ($\epsilon/M^{-1}\,cm^{-1}$) 385 sh (4900), 289 (44 000), 208 (23 000). Anal. Calcd for $C_{20}H_{30}F_{12}Fe_2P_2S_4$: C, 30.01; H, 3.78. Found: C, 30.18; H, 4.26.

Results and Discussion

Electrolytic oxidation of brown $[Cp'_2Fe_2S_4]$ at +0.30 V vs SCE in acetonitrile containing 0.1 M NH_4PF_6 as supporting electrolyte afforded a dark green diamagnetic dication salt $[Cp'_2Fe_2S_4](PF_6)_2$ (**2**) in 72% isolated yield. Spectroscopic data for the dication are consistent with the solid-state structure as determined by a single-crystal X-ray diffraction study[15] and also agree well with the data reported by Brunner et al. for $[Cp'_2Fe_2S_4]I_2{\cdot}2CH_2Cl_2$.[14]

The dication $[Cp'_2Fe_2S_4]^{2+}$ has a center of symmetry between the Fe atoms. Thus, two Cp′ rings take a staggered conformation to each other. Both of the bridging disulfur ligands lie in a plane almost perpendicular to the Fe–Fe axis. The Fe–Fe distance is significantly shorter (by 0.67 Å) than that in $[Cp'_2Fe_2S_4]$, but the length, 2.857 (1) Å, is still longer than the usual Fe–Fe single-bond lengths (cf. $Cp_2Fe_2(CO)_3SiHBu^t$, 2.614 (1) Å;[17] $Cp_4Fe_4S_4$, 2.618 (2), 2.644 (2) Å[18]). The S–S bond length, 1.983 (1) Å, is much shorter than those of $[Cp'_2Fe_2S_4]$ [2.055 (2) (doubly bidentate), 2.021 (2) (bidentate) Å] and those of the majority of disulfur-bridged complexes, which range from 2.01 to 2.15 Å.[19–23] The value observed for $[Cp'_2Fe_2S_4]^{2+}$ lies between the S–S single bond of α-S_8 (2.06 Å)[24] and the double bond of the S_2 molecule in the gas phase (1.89 Å).[25] Thus the S–S bond of $[Cp'_2Fe_2S_4]^{2+}$ is considered to take on a partial multiple bond character. Similar short S–S bond lengths have been reported for only a few disulfur-bridged complexes.[26,27] On the other hand, the distance between two disulfur bridges is 2.956 (1) Å, which indicates that there is no direct bonding interaction between them.

The neutral complex $[Cp'_2Fe_2S_4]$ has a doubly bidentate μ-S_2 ligand and a bidentate μ-S_2 ligand. Therefore, the structure of $[Cp'_2Fe_2S_4]^{2+}$ clearly demonstrates that the bidentate μ-S_2 ligand of $[Cp'_2Fe_2S_4]$ changed to a doubly bidentate μ-S_2 ligand in the course of two-electron oxidation. In the covalent model, the bidentate μ-S_2 ligand in $[Cp'_2Fe_2S_4]$ can be regarded as a two-electron donor to each iron atom, while the doubly bidentate μ-S_2 ligand can be considered as a three-electron donor to each iron atom. Thus, the each metal center of $[Cp'_2Fe_2S_4]$ satisfies the 18-electron rule, but after two-electron oxidation there are only 17 electrons on each of the iron atoms. At this stage, the change

Table I. ^1H NMR Chemical Shifts of the Signals for $A^+ + B^+$ and $A + B^{2+}$

$[A]_0$/mM	3.6	1.9	0.85
$[B^{2+}]_0$/mM	3.9	9.2	9.5
^1H NMR (CD_3CN)/δ_{ppm}			
$A + B^{2+}$ (diamagnetic)	1.60	1.60	1.59
$A^+ + B^+$ (paramagnetic)	−10.9	−15.5	−16.8

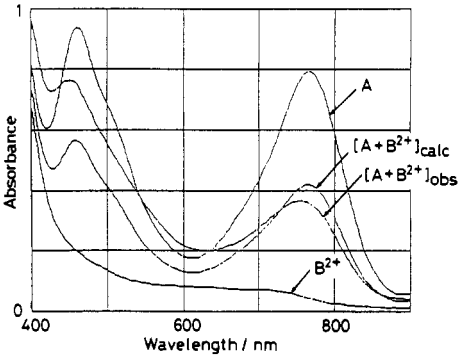

Figure 1. Electronic absorption spectrum of a 1:1 mixture of $[Cp'_2Fe_2S_4]$ (A) and $[Cp'_2Fe_2S_4](PF_6)_2$ (B^{2+}) immediately after mixing ($[A + B]_{obs}$) together with the spectra of A and B^{2+}, and the calculated mean spectrum of A and B^{2+} ($[A + B]_{calc}$). [A] = [B] = 0.18 mM at 25 °C.

of a bidentate μ-S_2 ligand to a doubly bidentate one allows it to satisfy the 18-electron rule again and stabilizes the complex. This is the first example of alteration of the coordination mode of μ-S_2 ligands accompanying electrode reactions, although a similar change has been observed in a few reactions of organovanadium disulfur complexes.[28,29]

For the discussion of redox behavior of the title compounds, we use the notation A and B, which represent the following structures of the Fe_2S_4 core, for species participating in the redox processes:

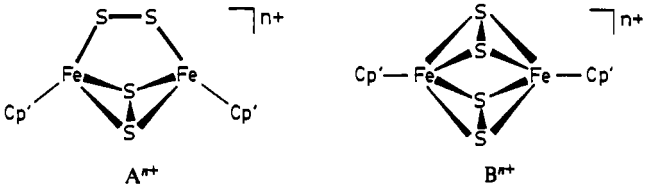

A^{n+} B^{n+}

n = 0, 1, 2

Namely, the complex or complex ion containing one bidentate μ-S_2 ligand and one doubly bidentate μ-S_2 ligand is represented by A, while that containing two doubly bidentate μ-S_2 ligands is represented by B. Additionally, the charge of the species is put as a superscript. Thus, for instance, the isolated complexes $[Cp'_2Fe_2S_4]$ and $[Cp'_2Fe_2S_4]^{2+}$ are represented by A and B^{2+}, respectively.

Electron-Transfer Reactions between A and B^{2+}. A ^1H NMR spectrum of a mixture of A and B^{2+} in CD_3CN solution shows not only a sharp singlet assignable to both A and B^{2+} (δ ca. 1.6 ppm) but also a broad signal at very high field. That there is only one singlet for two species, A and B^{2+}, might be explained either by a coincidence of their chemical shifts or by the coalescence of their signals due to a possible fast interconversion between A and B^{2+}. The broad signal can be assigned to the methyl protons of paramagnetic species A^+ and/or B^+ because of its large paramagnetic shift and the characteristic line width.[30] The chemical shifts of the signals for $A^+ + B^+$ and $A + B^{2+}$ are listed

(17) Tobita, H.; Kawano, Y.; Shimoi, M.; Ogino, H. *Chem. Lett.* **1987**, 2247.
(18) Schunn, R. A.; Fritchie, C. J., Jr.; Prewitt, C. T. *Inorg. Chem.* **1966**, *5*, 892.
(19) Wei, C. H.; Dahl, L. F. *Inorg. Chem.* **1965**, *4*, 1.
(20) Weberg, R.; Haltiwanger, R. C.; Rakowski-Dubois, M. *Organometallics* **1985**, *4*, 1315.
(21) Rauchfuss, T. B.; Rogers, D. P. S.; Wilson, S. R. *J. Am. Chem. Soc.* **1986**, *108*, 3114.
(22) Brunner, H.; Wachter, J.; Guggolz, E.; Ziegler, M. L. *J. Am. Chem. Soc.* **1982**, *104*, 1765.
(23) Brunner, H.; Meier, W.; Wachter, J.; Guggolz, E.; Zahn, T.; Ziegler, M. L. *Organometallics* **1982**, *1*, 1107.
(24) Müller, A.; Jaegermann, W.; Enemark, J. H. *Coord. Chem. Rev.* **1982**, *46*, 245.
(25) Meyer, B. *Chem. Rev.* **1976**, *76*, 367.
(26) Bolinger, C. M.; Rauchfuss, T. B.; Rheingold, A. L. *Organometallics* **1982**, *1*, 1551.
(27) Amarasekera, J.; Rauchfuss, T. B.; Wilson, S. R. *Inorg. Chem.* **1987**, *26*, 3328.
(28) Bolinger, C. M.; Rauchfuss, T. B.; Rheingold, A. L. *J. Am. Chem. Soc.* **1983**, *105*, 6321.
(29) Bolinger, C. M.; Rauchfuss, T. B.; Wilson, S. R. *J. Am. Chem. Soc.* **1984**, *106*, 7800.
(30) Ebsworth, E. A. V.; Rankin, D. W. H.; Cradock, S. *Structural Methods in Inorganic Chemistry*; Blackwell: Oxford, England, 1987; p 92.

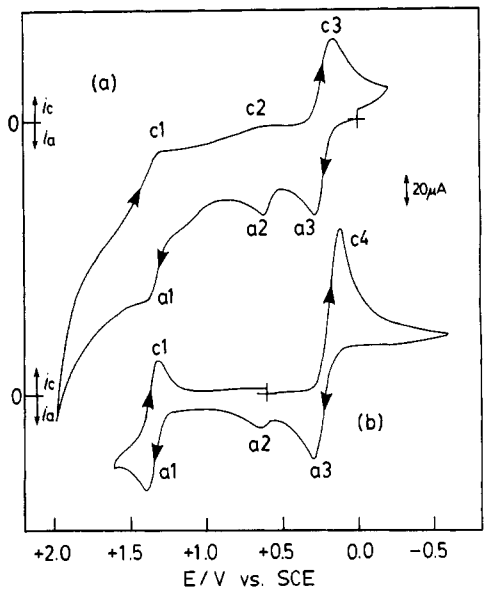

Figure 2. Cyclic voltammograms of (a) $[Cp'_2Fe_2S_4]$ (A) and (b) $[Cp'_2Fe_2S_4](PF_6)_2$ (B^{2+}) in acetonitrile at room temperature and sweep rate of 50 mV s^{-1}. [A] = 0.89 mM; [B^{2+}] = 1.05 mM.

Table II. Redox Potentials of A and B^{2+} (vs SCE) in Acetonitrile at Room Temperature[a]

	E_{pa}/V	E_{pc}/V	$E_{1/2}$/V	ΔE_p/mV
A	+1.39 (a1)	+1.30 (c1)	+1.35	90
	+0.70 (a2)	+0.60 (c2)	+0.65	100
	+0.30 (a3)	+0.19 (c3)	+0.25	100
	−1.30 (a6)	−1.39 (c6)	−1.35	100
B^{2+}	+1.39 (a1)	+1.30 (c1)	+1.35	90
	+0.68 (a2)			
	+0.30 (a3)			
		+0.15 (c4)		
	−1.30 (a6)	−1.39 (c6)	−1.35	90

[a] Sweep rate: 50 mV s^{-1}. E_{pa}: anodic peak potential. E_{pc}: cathodic peak potential. $E_{1/2}$: half-wave potential. ΔE_p: $|E_{pa} - E_{pc}|$.

in Table I for three different mixing ratios of A and B^{2+}.

The formation of paramagnetic species is further supported by the ESR spectrum of a 1:1 mixture of A and B^{2+} in a glass of acetonitrile–methanol at 77 K. It shows four intense signals: a pair of broad ones (g = 2.24 and 2.10) and a pair of sharp ones (g = 2.06 and 2.00).

These results are consistent with the existence of the electron-transfer reaction shown in eq 2.

$$A + B^{2+} \overset{K_1}{\rightleftharpoons} A^+ + B^+ \qquad (2)$$

$$K_1 = \frac{[A^+][B^+]}{[A][B^{2+}]}$$

To estimate how fast this equilibrium is attained, the electronic absorption spectrum was measured immediately after the solutions of A and B^{2+} were mixed (Figure 1). The electronic spectrum of the mixture was clearly different from the calculated spectrum for a 1:1 mixture of A and B^{2+} on the assumption that A and B^{2+} have no interaction. This spectrum does not show any change afterward. Therefore, the equilibrium is considered to be established at least within a few minutes at room temperature.

Cyclic Voltammetry of A and B^{2+} in Acetonitrile. Typical cyclic voltammograms of A and B^{2+} at room temperature are shown in Figure 2 (+2.0 to −0.5 V vs SCE) and Figure 3 (+1.0 to −1.5 V vs SCE), and their redox potentials are listed in Table II. Both A and B^{2+} show two quasi-reversible waves corresponding to the reduction of A to $[Cp'_2Fe_2S_4]^-$ (a6/c6; eq 3) and the oxidation of B^{2+} to $[Cp'_2Fe_2S_4]^{3+}$ (a1/c1; eq 4) at −1.35 and +1.35 V vs. SCE, respectively. However, no further study for these redox reactions have been attempted, so that our discussion will be

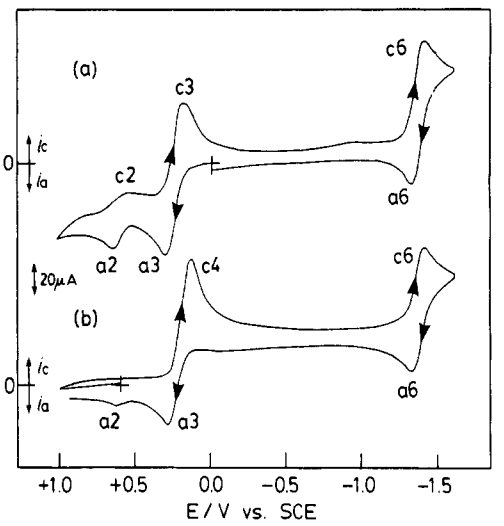

Figure 3. Cyclic voltammograms of (a) $[Cp'_2Fe_2S_4]$ (A) and (b) $[Cp'_2Fe_2S_4](PF_6)_2$ (B^{2+}) in acetonitrile at room temperature and sweep rate of 50 mV s^{-1}. [A] = 0.89 mM; [B^{2+}] = 0.78 mM.

restricted to the electrochemical events occurring within the potential range from +1.35 to −1.35 V vs SCE. In the electro-

$$[Cp'_2Fe_2S_4] + e^- \overset{E_{1/2} = -1.35\text{ V vs SCE}}{\rightleftharpoons} [Cp'_2Fe_2S_4]^- \qquad (3)$$

$$[Cp'_2Fe_2S_4]^{3+} + e^- \overset{E_{1/2} = +1.35\text{ V vs SCE}}{\rightleftharpoons} [Cp'_2Fe_2S_4]^{2+} \qquad (4)$$

chemical processes between two isolable species A and B^{2+}, we can assume at least four intermediate species A^+, A^{2+}, B, and B^+. We found that it is necessary to reckon with the existence of all these species to explain the cyclic voltammograms of A and B^{2+} under various temperature and sweep rate conditions, which will be discussed hereafter.

The cyclic voltammogram of A at room temperature shows a quasi-reversible oxidation wave (a3/c3) at $E_{1/2}$ = +0.25 V and a second, smaller oxidation wave (a2/c2) at +0.65 V vs SCE. The thin-layer cyclic voltammetry and coulometry of the first wave show that it corresponds to a one-electron oxidation. Thus the redox pair a3/c3 is assigned to eq 5.

$$A^+ + e^- \overset{E_{1/2} = +0.25\text{ V vs SCE}}{\rightleftharpoons} A \qquad (5)$$

The second wave is therefore tentatively assigned to the one-electron oxidation of A^+ (eq 6). The fact that this wave is

$$A^{2+} + e^- \overset{E_{1/2} = +0.65\text{ V vs SCE}}{\rightleftharpoons} A^+ \qquad (6)$$

appreciably smaller than the first oxidation wave (a3/c3) implies that a part of A^+ quickly converts to other species at room temperature, probably via the isomerization to B^+, while A^+ is quickly regenerated when A^+ is reduced at wave c3. At −36 °C, the height of the second oxidation wave becomes comparable to that of the first oxidation wave (Figure 4a). This reasonably indicates that the rate of conversion of A^+ to other species decreases when the temperature is lowered.

These observations and the high yield of B^{2+} by bulk electrolysis of A at +0.30 V vs SCE (=E_{pa} of A) strongly suggest the existence of the following ECE process: A^+ formed by the electrode reaction of A (eq 5) at room temperature equilibrates quickly with B^+, which is then oxidized at this potential to B^{2+}. At low temperature, perhaps the oxidation of B^+ to B^{2+} at the electrode becomes much less efficient partly due to the slowdown of diffusion, and the greater part of the equilibrium mixture of A^+ and B^+ survives until the potential is swept to the oxidation potential of A^+.

At a faster sweep rate (200 mV s^{-1}), a new small cathodic wave c4 was observed on the backward scan after the first oxidation (a3) (Figure 4b, dotted line). Wave c4 is assigned to the reduction of B^{2+} as will be shown in the next paragraph, and this is another good evidence for the existence of the ECE process. Wave c4

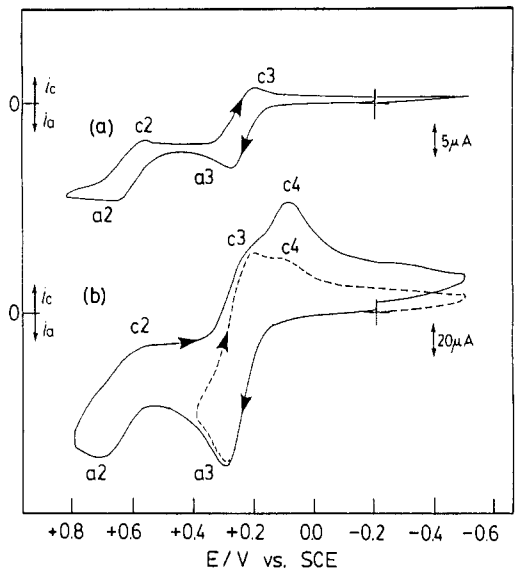

Figure 4. Cyclic voltammograms of $[Cp'_2Fe_2S_4]$ (A) in acetonitrile: (a) −36 °C, sweep rate 5 mV s^{-1}, [A] = 0.83 mM; (b) room temperature, sweep rate 200 mV s^{-1}, [A] = 0.75 mM.

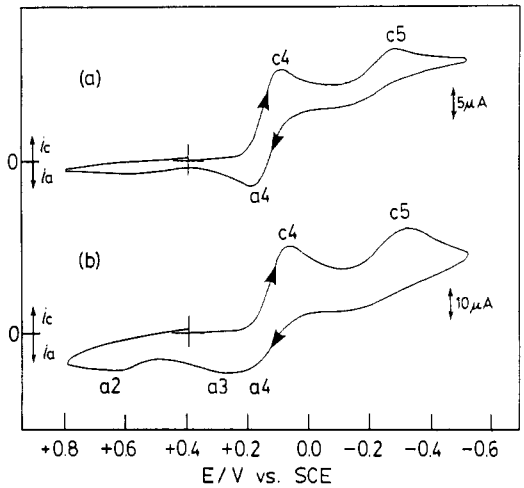

Figure 5. Cyclic voltammograms of $[Cp'_2Fe_2S_4](PF_6)_2$ (B^{2+}) in acetonitrile at −35 °C ([B^{2+}] = 0.90 mM): (a) sweep rate 10 mV s^{-1}; (b) sweep rate 50 mV s^{-1}.

becomes much larger when the potential sweep is switched after the second anodic wave, a2, appears (Figure 4b, solid line).

The cyclic voltammogram of B^{2+} at room temperature (sweep rate 50 mV s^{-1}) shows a large cathodic wave, c4, at E_{pc} = +0.15 V vs SCE and no further cathodic wave is observed until −1.35 V vs SCE (Figure 3b). From the height of this wave, this is interpreted to be a two-electron reduction of B^{2+}. On the other hand, the backward scan only shows the anodic waves for the oxidation of A (a3) and A^+ (a2) at +0.30 and +0.68 V vs SCE, respectively. Apparently, A is formed by the two-electron reduction of B^{2+}. No cathodic waves corresponding to a3 and a2, i.e. c3 and c2, were observed and the second anodic wave, a2, is smaller than that in the cyclic voltammogram of A. Namely, the intermediate ions A^+ and A^{2+} quickly and almost completely diminish in the B^{2+} solution probably via isomerization to B^+ and B^{2+}. On the other hand, in the A solution, certain amounts of A^+ and A^{2+} are continuously supplied by the electrode oxidation of A at potentials higher than +0.25 and +0.65 V vs SCE, respectively.

At −35 °C, however, the cyclic voltammogram of B^{2+} shows a clear second cathodic wave, wave c5, at E_{pc} = −0.30 V vs SCE assignable to the reduction of B^+ to B (Figure 5). This time a new anodic wave, a4, is also observed at +0.20 V vs SCE. This wave appears to pair with the cathodic wave c4, and therefore we assigned this pair to the one-electron oxidation of B^+ to B^{2+}

Scheme I

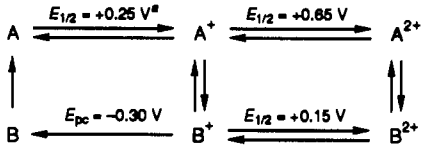

[a] All E measured vs SCE.

Scheme II

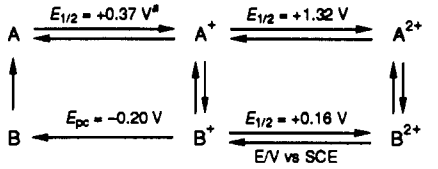

[a] All E measured vs SCE.

($E_{1/2}$ = +0.15 V vs SCE, ΔE_p = 100 mV). The observation of c5 and a4 implies that the equilibrium mixture of A^+ and B^+ has a sufficiently long life time for electrochemical detection under this condition. At the faster sweep rate (50 mV s^{-1}; Figure 5b), the oxidation waves of A^+ (a2) and A (a3) were also observed of which the latter might be attributable to A formed by the electron transfer between A^+ and B^+.

These behaviors invoke another ECE process: At room temperature, B^+ formed by the electrode reaction of B^{2+} at ca. +0.15 V vs SCE converts to its isomer A^+, which then immediately undergoes the second electrode reaction of eq 5 to give A. On the other hand, at −35 °C, the second electrode reaction becomes much slower, so that a considerable amount of A^+ and B^+ survives at the usual sweep rate to show the reduction (c5) and oxidation (a4) waves of B^+. It is known that in the ECE reaction when the second reduction occurs at significantly more positive potential and when the rate of the chemical reaction is sufficiently faster than the sweep rate, only a single two-electron wave is observed on a cathodic scan.[31,32] The electrochemical reduction of B^{2+} at room temperature corresponds to this case. In contrast to this, in the reduction of B^{2+} at −35 °C and also in the oxidation of A at room temperature, the rate of the second electrode reaction is comparable to or slower than the sweep rate. These observations show the domination of A^+ in the equilibrium between A^+ and B^+.

Consequently, the electrochemical and isomerization processes found to exist between A and B^{2+} are summarized in Scheme I.

The redox potentials among the dication, monocation, and neutral molecule of B-type species shift to the negative side compared to those of A-type species by ca. 500 mV. This is qualitatively explained by the stabilization of higher oxidation states in B^{2+} owing to the increase of the number of electrons contributed from two μ-S_2 ligands.

From the redox potentials given in Scheme I, we can estimate the equilibrium constant for eq 2. The difference between the potentials of A^+/A and B^{2+}/B^+ redox couples, −0.10 V, can be expressed as eq 7, where K_1 is the equilibrium constant for eq 2.

$$-0.10 = \frac{RT}{F} \ln \left(\frac{[A^+][B^+]}{[A][B^{2+}]} \right) = \frac{RT}{F} \ln K_1 \qquad (7)$$

Introducing T = 298 K, we obtain $K_1 = 2.0 \times 10^{-2}$. Therefore, the equilibrium of eq 2 lies far to the left.

Cyclic Voltammetry of A and B^{2+} in Dichloromethane. The electrochemical behavior of A and B^{2+} in dichloromethane is essentially the same as that in acetonitrile. However, we can find some important solvent effects on their cyclic voltammograms.

Most importantly, in the cyclic voltammogram of A at room temperature, the second oxidation wave a2 appears at +1.32 V vs SCE, ca. 600 mV more positive than that in acetonitrile (+0.70

(31) Bard, A. J.; Faulkner, L. R. *Electrochemical Methods Fundamentals and Applications*; Wiley: New York, 1980; p 461.
(32) Feldberg, S. W. *J. Phys. Chem.* **1971**, *75*, 2377.

V vs SCE). This phenomenon was already noticed by Brunner et al.[14] This large difference is hard to ascribe to solvation and implies a chemical difference in the species in the two solvents.

The electrochemical behavior of A and B^{2+} in dichloromethane is summarized in Scheme II.

Acknowledgment. We thank Prof. Masamoto Iwaizumi and Dr. Minoru Hanaya for the measurement of ESR spectra. The present study was supported by a Grant-in-Aid for Scientific Research, No. 63540469, from the Ministry of Education, Science and Culture, Japan.

Contribution No. 8388 from the Arthur Amos Noyes Laboratories, Division of Chemistry and Chemical Engineering, California Institute of Technology, Pasadena, California 91125

Electrochemical and Spectral Characterization of the "Square Scheme" for the Substitution of *N*-Methylpyrazinium Cation on the Ethylenediaminetetraacetate Complexes of Ruthenium(III) and Ruthenium(II)

Koiti Araki, Ching-Fong Shu, and Fred C. Anson*

Received January 24, 1991

The large difference in the affinity of *N*-methylpyrazinium cations for the ethylenediaminetetraacetate complexes of Ru(II) and Ru(III) produces a pattern of irreversibility in the electrochemical responses exhibited by these complexes. A combination of electrochemical and spectral measurements was utilized to obtain estimates of the equilibrium constants, rate constants, and formal potentials for a "square scheme", which characterizes the behavior of the system.

The replacement of the water molecule on the Ru^{III} center of $Ru^{III}(edta)OH_2^-$ (edta = ethylenediaminetetraacetate) by nitrogen heterocyclic ligands, L, can be readily followed electrochemically because of the shift in the formal potential of the Ru^{III}/Ru^{II} couple, which results from the substitution.[1,2] The unusual lability of the H_2O molecule coordinated to $Ru^{III}(edta)OH_2^-$[1,4] facilitates its replacement by ligands with greater affinities for Ru(III). The usual pattern is for the reversible couple $Ru^{III}(edta)OH_2^-/Ru^{II}(edta)OH_2^{2-}$ to be replaced by a new, reversible couple, $Ru^{III}(edta)L/Ru^{II}(edta)L$. However, in cases where the incoming ligand is bound only weakly to Ru(III) but much more strongly to Ru(II), an irreversible or quasi-reversible pattern can be encountered.[2,5,6] A particularly clear example of this type of behavior is provided by the interaction between $Ru^{III}(edta)OH_2^-$ and the strongly π-accepting *N*-methylpyrazinium cation (NMP^+). As is demonstrated in this report, the system adheres to the "square scheme" shown in Scheme I. The value of K_1 is much smaller than K_2 so that $E^f_{NMP} > E^f_{H_2O}$. Values of the two equilibrium constants and formal potentials as well as estimates of the rate constants governing the ligand-exchange reactions at the Ru(edta) center are given in this report. The values of the parameters obtained are consistent with the generally understood chemistry of the +3 and +2 oxidation states of Ru in which σ-acceptance and π-back-donation are important factors that influence the coordination of ligands to Ru(III) and Ru(II), respectively.

Experimental Section

Materials. $Ru(Hedta)\cdot 4H_2O$ was synthesized according to Mukaida et al.[7] from H_4edta and $RuCl_3\cdot nH_2O$. *N*-Methylpyrazinium hexafluorophosphate was prepared by metathesis from the commercially available iodide and was recrystallized three times from water. Other chemicals were analytical grade and were used as received. Glassy carbon electrodes (Tokai Chemical Co., Tokyo) were mounted with heat-shrinkable tubing as previously described.[8]

Scheme I

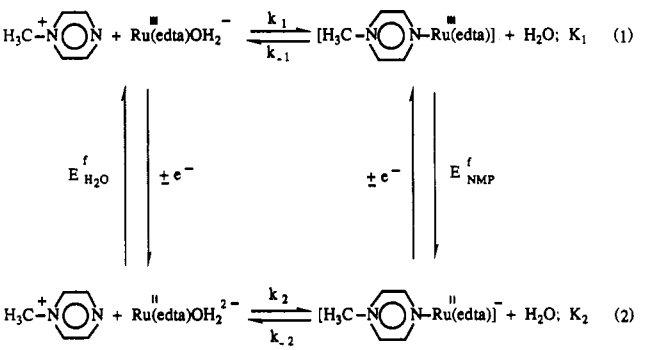

Apparatus and Procedures. Spectra were obtained with a Hewlett Packard 8450A spectrophotometer and 7225A plotter. Cyclic and rotating ring–disk voltammetry and normal pulse polarography were carried out with conventional instruments and two compartment cells. The rotating gold-disk–platinum-ring electrode (Pine Instrument Co.) had the following dimensions: r_1 = 0.38 cm; r_2 = 0.40 cm; r_3 = 0.42 cm. Glassy-carbon electrodes were polished first with 0.3-μm alumina followed by 0.05-μm alumina to produce a mirror-like finish. Polished electrodes were sonicated in pure water to remove residual alumina from their surfaces. Potentials were measured with respect to a Ag/AgCl (KCl = 1.0 M) reference electrode but are reported versus the standard saturated calomel electrode (SCE). All experiments were conducted at the ambient laboratory temperature, 22 ± 2 °C.

Results and Discussion

Reaction of $Ru^{III}(edta)OH_2^-$ with *N*-Methylpyrazinium Cations. The most labile form of the $Ru^{III}(edta)OH_2^-$ complex is present at pH values where the single uncoordinated carboxylate group is ionized.[1,2] The pK_A of this carboxylic acid is 2.4;[1,7] our experiments were carried out in acetate buffer solutions near pH 4.5. Solutions of $Ru^{III}(edta)OH_2^-$ (0.2 mM) are faintly yellow at pH 4.5, but addition of *N*-methylpyrazinium (NMP^+) produces the immediate development of an intense orange color. The color change is the result of a broad absorption between 500 and 420

(1) Matsubara, T.; Creutz, C. *J. Am. Chem. Soc.* **1978**, *100*, 6255; *Inorg. Chem.* **1979**, *18*, 1956.
(2) Toma, H. E.; Santos, V. S.; Mattioli, M. V. D.; Oliveira, L. H. A. Polyhedron **1987**, *6*, 603.
(3) Bajaj, H. C.; van Eldik, R. *Inorg. Chem.* **1988**, *27*, 4052; **1989**, *28*, 1980; **1990**, *29*, 2855.
(4) Ogino, H.; Shimura, M. *Adv. Inorg. Bioinorg. Mech.* **1986**, *4*, 107.
(5) Elliott, M. G.; Zhang, S.; Shepherd, R. E. *Inorg. Chem.* **1989**, *28*, 3036.
(6) Toma, H. E.; Araki, K. Submitted for publication in *J. Coord. Chem.*
(7) Mukaida, M.; Okuno, H.; Ishimori, T. *Nippon Kagaku Zasski* **1965**, *86*, 589.
(8) Oyama, N.; Anson, F. C. *J. Am. Chem. Soc.* **1979**, *101*, 3450.

0020-1669/91/1330-3043$02.50/0